# Accepted Manuscript

On the effect of surface roughness and material on the subcooled flow boiling of water: Experimental study and global correlation

M.C. Paz, M. Conde, E. Suárez, M. Concheiro

# On the effect of surface roughness and material on the subcooled flow boiling of water: Experimental study and global correlation.

M.C. Paz*, M. Conde, E. Suárez, M. Concheiro

School of Industrial Engineering – University of Vigo, Lagoas-Marcosende, 36310-E (Spain). (*) Corresponding author: cpaz@uvigo.es

## Abstract

In this paper, a new correlation based on experimental results for subcooled flow boiling of water at low pressure is proposed, preceded by a brief review on how the solid-fluid interaction has been dealt with in past correlations. The experimental sample comprises seven heating surfaces of different material (copper, aluminium and stainless steel) and roughness. The experimental facility is presented in detail and the surface morphology of each test specimen is analysed by means of an optical interferometer. The correlation is based on the assumption that the effect of material and roughness can be captured by means of modifiers of a general expression. The surfaces chosen in this work were selected to capture a broad range of industrial applications, and, though the correlation found fits well in the range of commercial and relatively high values of $R_a$ (up to 7 µm in the case of copper), further study is needed for larger values, as a discontinuity in the effect was observed, which has been previously determined by some authors. Thus, the proposed global correlation permits the calculation of the boiling heat flux taking into account, in addition to the more classical parameters such as pressure and bulk temperature, the effect of both the roughness and material of the wall heater, allowing its general use in low pressure applications such as those commonly found in the automotive industry.

## Keywords

Subcooled flow boiling, roughness, heater material effect, global correlation

## 1.    Introduction

Heat transfer is still a developing science in many fields of different industries such as nuclear refrigeration, micro-electronic cooling devices or automotive gas recirculation systems. One of the major goals at the current time is to achieve even more compact exchangers to save space and weight. In this context, heat transfer employing boiling mechanisms is a proper option to take into account. Nevertheless, despite being analysed in depth since the first half of the 20th century, nucleate boiling phenomenon is still unresolved at a global scale and no coherent theory has been established [1-6] mainly due to the great complexity of mass and energy transport mechanisms related with the two phases and the wide range of factors involved. This complexity is explained by the variety of characteristic length and time scales that take part in the process of bubble nucleation, growth, detachment, coalescence and collapse.

Probably the main advantage of nucleate boiling is achieving higher heat fluxes with relatively small increments of surface temperature. For example, in most conventional cases of the automotive industry as in EGR coolers or radiators without vapour separators or condensers, this heat transfer mechanism is used within reasonable limits avoiding a net generation of vapour, which may cause problems of vapour agglomeration in recirculating and top zones. In consequence, the heat transfer process must be run under subcooled conditions [7].

There are two main ways of approaching boiling characterisation, experimental studies and different levels of modelling techniques. Frequently, models dealing with nucleate boiling can be divided in two groups. The first group is comprised by mechanistic models that tackle the problem of identifying and modelling the physical parameters taking part in bubble nucleation phenomenon (e.g., bubble creation, growth, and departure diameter, nucleation frequency, nucleation site density and so on). The second type of models are normally called semi-empirical which instead of trying to reproduce the heat transfer at the wall by the individual contribution of the sub-processes involved, they directly relate it with the operational conditions and bulk properties of the materials involved.

As aforementioned and despite the big advances in recent years, no strong theoretical and global mechanistic model has been developed yet [5, 6]. As noted by several authors [5, 8] due to the vague knowledge of bubble formation at macro and microstructure levels, many of the past and recent predictive methods in practice are based on empirical and semi-empirical models.

Recently, the performance of mini and microchannels on boiling behaviour has received greater attention due to the increasing interest in compact heat exchangers employing this type of heat transfer technology. However, there are only a limited number of publications studying flow boiling and CHF from the experimental point of view [9-12]. Recently, Cikim [13] incorporated the effect of surface coatings on the boiling behaviour of this type of system. These works examine the same issues addressed in the present work, but the scales involved in the development of the bubbles compared to the scale of the channel require a specific approach to the process.

This work addresses the experimental characterisation of the subcooled nucleate boiling of water at low pressure as an experimental contribution towards the formulation of new semi-empirical correlations to be applied for the calculation of the flows normally found on a heat exchanger employed in the automotive industry. The proposed methodology will try to reach a general expression for the most common materials (copper, aluminium and stainless steel) and their regular range of surface finish in the nucleate boiling regime.

## 2.    Background

### 2.1.    Review of boiling heat transfer parameters

When trying to explain the different aspects that are known to have significance on boiling heat transfer, the common practice using semi-empirical models is to separate the influences into independent factors. Additionally, to improve the accuracy of the model, crossed dependences between some of these factors should be taken into account.

Probably since the first research on surface boiling, the main role that surface finishing and roughness play in nucleation characteristics has been assumed. For instance, in the early sixties, Berenson [14] noted the importance of including surface roughness in boiling analysis but focusing in surface finishing and in the morphology of the nucleation cavities. Moreover, assuming the fact that the surface finishing technique does not essentially affect other properties of the material such as ductility, malleability or hardness, thermal properties of the material have an apparent role in the transient conduction process near a nucleation site.

Marto and Rohsenow in 1965 [15] analysed previous studies of several authors and emphasised at least three effects concerning the surface that have a considerable effect on bubble nucleation: surface roughness, surface material and wetting characteristics of the solid-liquid combination (in terms of oxidation layer, additives and impurities of the liquid and even in the state of stress of the system). In their research, they give, upon several simplifications, a stability model where the instability is caused by sudden deactivation of active nucleation sites. They developed their research studies for sodium, much more instable than ordinary fluids,

and concluded that increasing the diffusivity of metal surface as well as effusivity leads to a higher stability. Also, the same effect is derived for the heat flux. They encountered that roughness affects the form of the boiling curve not only at the early stages of incipient boiling but also over the range of stable nucleation. Other effects such as aging, hysteresis, chemical treatment of the surface, porous coating and of course pressure and fluid properties, also have a significant influence.

Tachibana et al. [16] have found that the critical heat flux point is strongly affected by the thickness of the heater using flat plates as test sections and suggest a new correlating parameter in terms of the heat capacity per unit of area (i.e.: $\delta_w \cdot \rho_w \cdot c_w$). They also noted oxidation and precipitation processes to have influence in CHF. According to Tachibana et al., at least a value of 0.88 mm is needed to be free of heat capacity effects in the case of stainless steel plates. Guglielmini and Nannei [17] report important effects on CHF below a threshold value for the wall thickness and give a correlation based on the wall's thermal effusivity for calculating the aforesaid value. Later Golobič and Bergles [18] reaffirm the thickness dependence in CHF together with the conductivity and thermal capacitance of the wall. Another example is the correlation proposed for calculating the CHF point by Watwe and Bar-Cohen and modified later by Arik and Bar-Cohen [19] which make use of the parameter $\delta_w \cdot (\rho_w \cdot c_w \cdot k_w)^{0.5}$, similar to the approach used in this work.

In fact in 1969, Sernas and Hooper [20] already considered both liquid and solid effusivity dependence in heat transfer and bubble growth rate calculations under different assumptions for the size and nature of the microlayer under the bubble; their conclusions were used later by Unal [21] to give expressions for the maximum bubble diameter and other nucleation parameters. As a continuation of this work, Benjamin and Balakrishnan [22] define a model of pool boiling with an expression for the nucleation site density in terms of the ratio of wall to fluid effusivities; the contact angle as a function of roughness, surface tension and pressure; the wall superheat and the viscosity of the fluid ( i.e., the Prandtl number). They precisely remark the important role of the viscosity in pool boiling heat transfer [23] and the relative role that roughness plays in bubble nucleation, that is, that the same surface can be "smooth" or "rough" depending on the fluid, somehow bringing Rohsenow's parameter [24] up for the fluid-surface interaction.

However, surfaces evolve during their service, especially under boiling operations, hence their characterisation prior to their use is generally not sufficient to predict their long-term behaviour. The sum of the processes leading to this has been commonly called ageing. Sterman and Vilemas [25] remark the antagonist effect of ageing in CHF found depending on the author taken into consideration. They show that the CHF point is closely related to surface wettability changes due to impurities, deposition, and conditions of the surface. As concluded by Steiner et al. [2], ageing is a decisive parameter and very difficult to analyse especially in water experiments due to the complexity of chemical and physical sub-processes which are very difficult to measure. They also observed the microstructure of the surface to be the main long-term representative roughness parameter in contrast to the time limited effects of the macrostructure.

Chowdhury and Winterton [26] concluded that wettability is a critical factor in boiling heat transfer. This important dependence was later called on by Kolev [27] to justify the large spread in experimental data achieved by different researchers. Working with aluminium, Chowdhury and Winterton proved ageing effects on well-polished parts to be conclusive about the reduction of the contact angle and the consequent rise on HTC, as some authors stated before. Ageing and its effect on contact angle in aluminium is often attributed to surface oxidation. Similarly, the work of Hong et al. [28] corroborates the reduction of the contact angle with surface oxidation due to the change in the surface's morphology. Recent studies of Lee et al. [29] highlight the role of both surface tension and contact angle in looking up methods for heat transfer enhancement.

An early review on how the different factors affect boiling can be found in [30]. Cooper suggests a roughness dependence which also depends on pressure as he found that the roughness effect was greater at low pressures. Regarding the material of the heater, he did not find any strong dependence with the conductivity of the material so he lumped this dependence together with the heater's shape into a material constant. On the other hand, recently, Zou and Jones [31] claimed similar values for nucleation site density, diameter and bubble growth rate in copper and stainless steel surfaces, and appealed for thermal properties, mainly conductivity, to justify observed differences with HTC values.

The intricacy of fluid-surface coupling has been noted by several authors such as Pioro et al. [32, 33] and Saiz-Jabardo et al. [6], remarking the difficulty in introducing the solid-fluid–vapour interaction in any model or correlation due to the interdependence of different factors and the complexity of measuring techniques. As a consequence, factors such as oxidation, surface fouling and contamination, surface finishing and even manufacturing process effects are very complex to measure. Pioro et al. blame these uncertainties on the lack of accuracy and the relatively big errors of boiling models. Also, they encountered the heat transfer process to be dependent of thermal conductivity and thermal absorption of the wall material

Many present and past authors have found direct effects of surface roughness on HTC [14, 26, 34, 35] arguing that higher roughness has more potential nucleation sites to be active enhancing the heat transfer process. This statement is true provided that the surface finish and morphology is similar for the specimens under study and the average roughness does not exceed certain limits. For example, Luke [36] has concluded that rolled surfaces have better values for HTC than sandblasted surfaces, even having lower values for average roughness. He explains this behaviour by the large directional crevices present in rolled surfaces.

In this context studies with artificial cavities as in [37] prove that spacing and pattern cavities have also an influence on bubble diameter, nucleation frequency and wall temperature distribution. Related to this subject, Pike-Wilson et al. [38] and McHale and Garimella [39] prove the necessity of new functional roughness characterisations instead of the classical ones to better explain HTC-roughness dependencies. This become even more necessary when considering the experimental results of some authors about an observed upper limit of the roughness for the maximum HTC beyond which it commences to diminish [6, 23].

Recently and focusing on the location of the critical heat flux point under pool conditions, M. Arik et al. [40] in a comprehensive study, summarises the boiling dependence into two main categories of parametric effects, one concerning the heater and the other dealing with the working fluid. On the former group they remark about the thermal properties, characteristic length, surface characteristics (at macro, micro and nano levels) and surface orientation of the heater, while on the latter the main effects are due to pressure, bulk temperature and thermo-physical properties of the fluid (pure, mixture or enhanced with nanoparticles).

Consequently, it can be concluded that the effect of material and surface morphology on boiling behaviour is an open issue that needs further research. It has been clearly established that average parameters such as Ra, though extensively employed, are not sufficient to explain the boiling curves of different surfaces, and other material related parameters such as effusivity have demonstrated certain levels of significance but still are considered deficient to agglomerate the whole influence of the materials on their boiling response. The work presented here, tries to contribute in this task with a new set of experimental values of the boiling performance of different materials with different surface morphologies.

## 2.2.    Review of boiling models

Historically, one of the main shortfalls of the widely used Chen's model [41] is the non-dependence on the heater material and surface roughness. Rohsenow [24] many years before, had considered this effect adding an empirical constant depending on the heating surface-fluid combination to its pool boiling correlation in order to capture surface roughness effects, wetting properties or cleaning conditions of the surface. Precisely, in 1998, Pioro [42] made a review of published constants for the Rohsenow correlation and performed some new tests calculating values for the Rohsenow constant for various surface-fluid combinations, heater morphology and surface conditions [e.g., wire, plate, corrosion grade, finishing, coating and so on]. Pioro's work was complemented in 2004 by Saiz-Jabardo et al. [43] evaluating Rohsenow's correlation for several halocarbon refrigerants in cylindrical surfaces of different materials and giving an expression for the fluid-surface characteristic constant in terms of surface roughness

Cooper [30] in 1984 came up with the idea of using reduced properties (i.e., $p_r$ and $T_r$) and molar mass instead of others which could be difficult to measure. He argued that, in fact, all the other properties could be given by functions of the former with acceptable accuracy for this purpose, even further due to the wide error bands given by the correlations up to date.

$$\frac{h_{nb}}{q^{.0.67}} = C_w \cdot p_r^{0.12-0.2\log_{10}R_{p,old}} \cdot \left(-\log_{10}p_r\right)^{-0.55} \cdot M^{-0.5} \quad (1)$$

Moreover, the correlation suggested by Cooper [Eq. (1)] also for pool boiling, takes account of heater surface roughness, material, heater shape and orientation even though these effects except roughness are lumped into an empirical constant $C_w$.

A year after Cooper in 1985, Gungor and Winterton [44] developed a general correlation for modelling flow boiling in tubes using the asymptotic model introduced later [Eq. (10)] with n=1. They proposed the Cooper correlation for the nucleate boiling term together with the Dittus-Boelter expression for the purely forced convection contribution. For the enhanced factor $E_F$, they extended its dependence to the boiling number in addition to the Martinelli number as Chen [41] had stated before. Due to this new dependence, they had to redefine Chen's suppression factor but the basic structure was maintained. They also gave a correction in terms of the Froude number for horizontal tubes as well as the critical value for tube gap in the case of annuli to choose the characteristic perimeter when calculating the hydraulic perimeter. Again, they concluded with the adequacy of using reduced properties in place of ones more difficult to measure such as surface tension, after evaluating another Rohsenow-based [45] model for the estimate pool boiling term. Later in 1990, Liu and Winterton [46] justified the convenience of using n=2 in the asymptotic model modifying again the S and $E_F$ expressions in [44]. They made a deviation comparison for both the saturated and subcooled boiling of Shah [47], Gungor and Winterton [44], Chen [41] and the new proposed correlation, remarking the bad performance of Chen's model for the saturated boiling regime with some new refrigerants, especially argon or alcohols

Despite the considerable deviation of Chen's model for some cases as stated before, its simple additive structure together with the independence of HTC with q" (i.e., Bo number), are the reasons why this model is still widely used in many industries and computer models. This is particularly interesting when dealing with well-known fluids and small changes in operation conditions, obtaining good results carrying out little modifications on $E_F$ and/or S factors. A good example of this trend can be found in the work of Torregrosa et al. [48], choosing the mentioned Chen model as a reference and modifying the suppression factor in terms of the Prandtl number.

Another successful strategy in boiling modelling is the one assumed in the VDI heat atlas [49]. It consists of identifying the most significant factors among the possible dimensionless groups formed with common variables and properties in which boiling

depends on. The idea is clearly explained by Stephan et al. in [45]. Among other properties, they also came across the necessity of including the heater material properties, especially for cryogenic refrigerants. The initial VDI concept was revisited later by several researching work, e.g., [50-54] and is still under continuous improvement by the time new experiments come to light. The more up-to-date VDI model is reviewed in [55] and the implementation for water as coolant fluid is given in Eqs. (2-7)

$$\frac{h_{nb}}{h_{nb,0}} = F_q \, F_{p*} \, F_f \, F_{wr} \, F_{wm} \tag{2}$$

$$F_q = \left(\frac{q''}{q_0''}\right)^n \quad where \quad n = 0.9 - 0.3 \, p^{*0.15} \tag{3}$$

$$F_{p*} = 1.73 \, p^{*0.27} + 6.1 \, p^{*2} + 0.68 \frac{p^{*2}}{1 - p^{*2}} \tag{4}$$

$$F_f = \left(\frac{P_f}{P_{f,ref}}\right)^{0.6} \quad where \quad P_f = \left[\sigma^{-1}\left(\frac{dp}{dT}\right)_{sat}\right]_{p*=0.1} \tag{5}$$

$$F_{wr} = \left(\frac{R_a}{R_{a,0}}\right)^{2/15} \tag{6}$$

$$F_{wm} = \left(\frac{\rho \cdot c \cdot k|_w}{\rho \cdot c \cdot k|_{Cu}}\right)^{0.25} \tag{7}$$

The dimensionless functions F are independent and stand for the identified boiling dependences. $F_q$ and $F_{p*}$ cover the dependence of HTC with heat flux and pressure, respectively whereas $F_f$ stands for the influence of the thermophysical properties of the fluid. As seen in Eqs. (6) and (7), $F_{wr}$ and $F_{wm}$ model the heater material dependence in terms of roughness and effusivity. This group of functions sets a reference point for each of the variables, shown in Table 1, to obtain the dimensionless parameters. The values of $P_f$ and $p_c$ for water are 1.268 $(\mu m \cdot K)^{-1}$ and 220.64 bar respectively.

## 3.    Experimental setup

### 3.1.    Test bench and measure equipment

The experimental bench (Fig. 1) designed for carrying out the boiling test is comprised by two parts: the study section (13) and the piping and other auxiliary elements allowing a controlled flow in terms of pressure, velocity and temperature of deionised water.

The study section Fig. 2 consists of a 25x20x1200 mm rectangular channel made of AISI 316 with three polycarbonate windows and the test part (26) centred at the bottom of the passage. The test part, with an upper surface of 50x10 mm in touch with the water, is insulated from the rest of the system by a PTFE skin (25) to avoid undesired heat losses. The size of the PTFE isolation skin has been selected to reduce the lateral leakage of heat below the level of uncertainty of the system. Embedded in a copper heating block (29) that is insulated with glass wool are four heating cartridges (30) that achieve a total power of 2000 W.

The measurement of the temperature is performed using 6 thermocouples (k-type, class-2 tolerance, 0.5 mm diameter and 0.03 s response time), which are located on the test part as shown in Fig. 3.

Data acquisition comprises of a data acquisition card acquiring at 1 kHz values for the temperatures (bulk and hot part), volumetric flow and pressure. This kind of experimental setup has been successfully employed by other researchers such as Celata et al. [56], Ramstorfer et al. [57] and Ribatski et al. [58].

For obtaining the topography of test part surfaces a Wyko NT1100 optical profiling system was used.

### 3.2.    Test part characteristics

The experimental sample is formed by seven test parts in which manufacturing characteristics and other properties are shown in Table 2. Each of the test parts is completely made of the test material but the stainless steel one (SS-L), which consists in a copper base part with an AISI 316 thin strip of 0.5 mm thickness attached to its upper surface by brazing. This manufacturing method was selected to avoid the big amount of installed power needed to heat a hypothetical solid part made entirely from steel and the unmanageable expected temperatures. One of the consequences of this particular solution concerns the effusivity value to be

used. As aforementioned, the ratio of the effusivity of the solid material and the fluid is a common factor in the characterisation of the effect of the heater. This is based on the fact that the movement of the liquid to fill the void space generated by a bubble leaving the wall is depicted as a sudden contact of two bodies at a different temperature. Theoretically if two semi-infinite solids A and B with initial temperatures $T_A$ and $T_B$ are suddenly put in contact, the temperature of the common interface remains constant over time and can be theoretically calculated [59]. Hence, the effective effusivity of the surface can be derived from a test were it is suddenly put in contact at a different temperature with a known material. In this case, resolving the heat equation for this transient problem, the thermal effusivity of solid B in terms of the interface temperature, thermal effusivity of solid A and the initial temperatures for blocks A and B can be derived from Eq. (8).

$$(\rho \cdot c \cdot k)_B^{0.5} = \frac{(\rho \cdot c \cdot k)_A^{0.5} \left( T_{A,initial} - T_{interface} \right)}{T_{interface} - T_{B,initial}} \qquad (8)$$

To estimate an approximate value for the SS-L part a one-dimensional simulation has been performed given water values for the properties of solid A and modelling the 0.5 mm strip in AISI 316 with the rest of the semi-infinite body in copper. The resulting value of this mixing thermal effusivity rises up to 35,100 $J \cdot m^{-2} \cdot K^{-1} \cdot s^{-0.5}$ whereas the value for steel at 130 °C is about 7,220 $J \cdot m^{-2} \cdot K^{-1} \cdot s^{-0.5}$.

The seven different test sections were manufactured to produce different morphologies and levels of roughness with three different materials: copper (Cu), aluminium (Al) and stainless steel (SS). Their levels of roughness are coded as low (L), medium (M) and high (H) by comparison with the common grades of roughness regularly employed at the industrial level.

The morphology of the surfaces has been studied by means of a white light interferometer, before and after running the experiments. The images obtained and a sample of the profile measured over two perpendicular lines randomly chosen, are shown in Fig. 4.

The smoothest copper and aluminium surfaces (Cu-L and Al-L) were produced by manually sanding and polishing to generate a roughness in the range of smooth industrial tubes and plates. Their optical 3D profilometries show that before the tests, their topographies have peaks and valleys well below 1 µm. Some directionality can also be observed in the direction of the flow. The other copper (Cu-M and Cu-H) and aluminium surfaces (Al-M and Al-H) were produced by EDM (Electrical Discharge Machining), which produces different degrees of roughness with no preferred direction. Their morphologies are clearly characterised by deep valleys and peaks that are quite evenly distributed all over the surface. Cu-M requires special mention, as it combines the machining processes of Cu-L and Cu-H. In this case, as the range of morphologies generated by EDM on copper did not produce a significant difference in their roughnesses, Cu-M was subsequently sanded to reduce its roughness to produce a medium level value. Its topography clearly shows a flat surface with several randomly distributed valleys. Finally, due to the low conductivity of the stainless steel, its test part (SS-L) could not be fully made of it; thus, this test part instead consists of a copper base part with a thin AISI 316 strip brazed to the copper. The strip of stainless steel is a section of a cold-rolled tube whose rolling direction is the same as the flow.

Fig. 4 also shows a clear modification of the surface's micro-roughness due to the processes commonly known as ageing that may involve erosion, deposition, oxidation and corrosion. As mentioned, the processes grouped as ageing are not well understood and, in general, cause the boiling curve to drift towards higher wall temperatures for a given heat flux. Some authors have proposed that the influence of ageing on boiling is mainly due to the modification of the wettability of the surface, but other researchers have proposed different mechanisms such as the modification of the micro-morphology of the cavities trapping vapour, the loss of material due to erosion, or the generation of a low-conductivity layer of oxide on top of the experimental specimen. To avoid the overlapping of ageing during the tests, every surface was exposed to intense boiling for tens to hundreds of hours. Hence, all of the data provided in this work correspond to tests performed after each surface has achieved a level of ageing that no longer affects its boiling curves.

### 3.3. Array of experiments

The independent variables considered for every test performed with each test part were system pressure, bulk temperature and bulk velocity. The selected running test points are shown in Table 3.

## 4. Correlation of the results

### 4.1. Widespread flow boiling model structures

One of the first empirical models to estimate flow boiling heat transfer is due to Mc. Adams et al. [60]. In 1945, they proposed to separate the heat transfer process into two parts by a characteristic temperature named transition temperature. Before this temperature, i.e., the macro-convective dominant region, the Sieder-Tate expression with a re-calculated constant was used. For the subcooled boiling region uses the potential approach given in Eq. (9).

$$q'' = C' \cdot \Delta T_{sat}^{3.86} \qquad (9)$$

The adjusting parameter C´ value depends on the amount of dissolved gas existing in the flow. This kind of potential structure is frequently appealed when a locally scoped model is needed with no big variations in the operation conditions. Later, in order to make a smooth transition between the two parts outlined by Mc. Adams et al., Rohsenow [24] suggested the idea commonly known as the superposition model, developed a few years later by Chen [41], which has been widely assumed and modified up to current days [44, 48, 61-63]. This kind of model assumes the total heat flux to be calculated as the contribution of two factors, the first one standing for the macro convective heat flux and the other that stands for the nucleate boiling heat flux or micro convective component. A more general form of this strategy is the so called power-law interpolation [Eq. (10)] or asymptotic model already mentioned before.

$$q_{tp}^{''n} = q_{fc}^{''n} + q_{nb}^{''n} \qquad (10)$$

These models generally introduce factors that apply one or both heat fluxes to better approach a physical phenomenon. For instance, the widely used aforementioned Chen [41] model provided by Eq. (11), in which n=1 (i.e., a simply additive model), introduces an enhancement factor $E_F$, to correct the Re number of the flow due to the presence of vapour bubbles, which is almost always omitted in the subcooled regime, and a S suppression factor that diminishes the boiling heat flux as the flow velocity increases.

$$q_{tp}^{''} = E_F \cdot q_{fc}^{''} + S \cdot q_{nb}^{''} \qquad (11)$$

The reason for the existence of S is that $q''_{nb}$ is meant to be used in pool boiling (developed by Foster and Zuber in 1955). In general, the value for n in Eq. (10) depends on how the individual expressions manage to estimate the contribution of the two heat fluxes or alternatively the HTCs in different test conditions. In this context, Kutateladze [64] justifies the use of n=2, Steiner and Taborek [65] find n=3 as the best value and Shah [47] choose the larger of both values, that is n=∞. The conceptual model given in Eq. (10) has the advantage that the engineer or designer can incorporate the set of correlations which best estimate their particular problem for the two contributions together with the suppression and enhanced factors.

Another model structure that differs conceptually from the one presented in Eq. (10) is to estimate the two phase heat transfer from the pure convective coefficient modified by a function *(Bo)*, as shown in Eq. (12), when the ONB point is reached. This approach was used by Shah [66] and Kandlikar [67] to model subcooled boiling.

$$q_{nb}^{''} = \phi \cdot h_{fc} \cdot \Delta T_{sat} \qquad (12)$$

## 4.2. Proposed model

The model presented here assumes the structure given in Eq. (10) with n=2. For the nucleate boiling contribution the VDI pool boiling given in Eqs. (2-7) modified by a suppression factor given in Eq. (13) has been employed.

$$S = \frac{1}{1 + 0.055 \cdot Re^{0.2}} \qquad (13)$$

There has been no consideration of any enhancement factor provided the fact that the boiling regime is developed under subcooled conditions.

Additionally, instead of the parameter $R_a$ for the characteristic roughness height, the areal parameter $S_a$ (defined according to ISO 25178-2) and shown in Eq. (14) has been used as an input in Eq. (6) to average the effects of surface anisotropy. The value for the forced convection contribution was taken from the experimental data fitting process.

$$S_a = \frac{1}{S} \iint_S |z(x,y)| \, dx \cdot dy \qquad (14)$$

The heat exchange is then calculated with the following expression [Eq. (15)]

$$q''^2 = \left[ h_{fc} \cdot (T_w - T_b) \right]^2 + \left[ S \cdot h_{nb} \cdot (T_w - T_{sat}) \right]^2 \qquad (15)$$

where $h_{nb}$ and S are given by Eq. (2) and Eq. (13) respectively. In the interest of clarity, the modified method for calculating $h_{nb}$ is shown again in Table 4.

## 5.    Results

In Fig. 5 the model performance for all test points and all parts is shown. Red points belong to part Al-H for which the model fails due to the observed backward trend for the highest surface roughness. As seen in Fig. 6, curves for the Al-H test part are sandwiched by the curves corresponding to Al-L and Al-M parts or they are even below them. This behaviour is inconsistent with the model response when varying roughness [Eq. (6)].

An example of the model response to changes in roughness height for copper is shown in Fig. 7 while the model output for the three different materials is shown in Fig. 8. It can be inferred analysing the experimental data for the stainless steel part in this chart, that the base copper material below the thin strip of steel must have many influence since the steel data are between copper and aluminium. This would be inconsistent with the fact of assigning the lowest steel effusivity value to the part as it was made entirely from steel.

In order to evaluate the global goodness of the presented model, a comparison with some other subcooled boiling models has been performed. The selected models are: Chen [41], Shah [66], Liu and Winterton [46] and Kandlikar [67]. The comparative result chart is shown in Table 5. It can be observed that the presented model obtains the best error value for almost all test parts. For the reason that has been mention before, the model output for the Al-H test part is clearly overestimated. In the case of the stainless steel part, the presented model is very slightly worse than the Chen and Liu-Winterton ones. A further validation of the proposed model would require its application to the experimental data available in the literature in the same range, i.e., low pressure, subcooled flow boiling. Unfortunately, the available experimental databases generally employed as references [62, 68-71] do not provide the necessary surface morphology information to apply the proposed correlation, and its generality has therefore not yet been assessed.

Nevertheless, the relatively best performance of Chen's model in the case of stainless-steel, might reveal itself little promising at higher boiling power due to the low slope of the model output that does not seem capable of following the experimental rising trend, as seen graphically in Fig. 9 (D and E). In fact these charts show the graphical output for some test points, parts and models and they clearly reveal the necessity of a model correction mainly in terms of wall roughness and material. As an example, in the Kandlikar model that does not include any correction, the heat flux for the copper smooth parts (A to C) is highly overestimated while it is underestimated in the case of the roughest ones (G to I). Neither does the widely used Chen model include any heater wall correction so it mainly fails in a greater or lesser extent with the roughest copper and aluminium parts (G to L). Concerning the Liu-Winterton model the factor accounting for the roughness of the wall, the same as in the Cooper's expression [Eq. (1)], greatly overestimates the effect in the case of the Cu-H parts (G to I).

Another remarkable observed issue was the big error achieved with the Kandlikar model in the case of the lowest Re number points that obviously swell the global statistical error figures, due to the inclusion of the convective HTC in the fully developed boiling region.

As seen in both Table 5 and Fig. 9 (J to L), there are no data about the output curves for the Liu-Winterton model in the case of aluminium parts. This unavailability is because no value for the wall constant in the case of aluminium is given either in [46] or in the original expression by Cooper [30] in which the model is based on.

## 6.    Conclusions

Experiments on the subcooled flow boiling of water at low pressure over a flat plane were conducted with seven different heating surfaces of three materials (copper, aluminium and stainless steel) and different levels of roughness. The focus of the study was the influence of the surface morphology and thermal properties on the boiling curve.

It has been seen that a unique parameter of roughness measurement ($S_a$) is not enough for the characterisation of a boiling model in terms of surface morphology, though it seemed to produce better characterisation than the commonly used $R_a$, whose directional nature is unsuitable for dealing with a multiscale phenomenon such as boiling. Further study and the inclusion of other morphological parameters is needed to achieve a better phenomena understanding and modelling. Moreover, this new characterisation is especially important in the case of highest roughness and the observed trend reversing with the roughness-boiling heat couple. Nevertheless, for most commercial surface finishing methods and with admissible accuracy values, it might be enough for a model comprising of both a roughness correction factor in terms of the parameter $S_a$ and a material factor in terms of the wall material effusivity as the one presented here, following the VDI heat atlas strategy. This new model has been shown to improve the prediction of heat flux vs. wall temperature in the range of pressure, velocity and subcooling tested in this work.

In addition, in the case of coated and sheathed surfaces with presumably thin thickness for the outer layer, it is necessary to accommodate a correction in the value of the effusivity to be used for the wall material.

**Nomenclature**

Bo     boiling number

c      heat capacity [$J \cdot kg^{-1} \cdot K^{-1}$]

C'     Mc. Adams constant in Eq. (9)

$C_w$     Cooper constant in Eq. (1)

$E_F$     enhanced factor in Eq. (11)

F      VDI model functions in Eqs. (2) to (7)

h      heat transfer coefficient [$W \cdot m^{-2} \cdot K^{-1}$]

k      thermal conductivity [$W \cdot m^{-1} \cdot K^{-1}$]

M     molar mass [$kg \cdot mol^{-1}$]

n      exponent in the asymptotic model in Eq. (10)

p      pressure [Pa]

$P_f$     characteristic boiling parameter of the fluid [$K^{-1} \cdot \mu m^{-1}$] in Eq. (5)

p*     reduced pressure

q''     heat flux [$W \cdot m^{-2}$]

$R_a$     arithmetic mean roughness height [$\mu m$]

$R_{p, old}$     $= R_a/0.4$ (DIN 4762) [$\mu m$]

Re     Reynolds number

S      suppression factor in Eqs. (11), (13), (15)

$S_a$     arithmetic mean surface height [$\mu m$]

T      temperature [K]

Abbreviation:

AT     after tests

BT     before tests

CHF     critical heat flux

HTC     heat transfer coefficient

ONB     onset of nucleated boiling

Greek:

δ      thickness [m]

Δ      increment

ρ      density [$kg \cdot m^{-3}$]

       boiling function in Eq. (12)

Subscripts:

b       bulk

c       critical state

Cu      copper

fc      forced convection

min     minimum

max     maximum

nb      nucleated boiling

r       reduced state

sat     saturated state

sub     subcooled

tp      two phase

w       wall

## Acknowledgements

## References

[1]      P. Stephan, Introduction, Second English edition ed., V. D. I. V. V. und Chemieingenieurwesen (GVC), Springer-Verlag, 2010, pp. 757-792.

[2]      H. Steiner, G. Brenn, F. Ramstorfer and B. Breitschadel, Increased cooling power with nucleate boiling flow in automotive engine applications, New Trends and Developments in Automotive System Engineering, 2011, pp. 249-272.

[3]      G. Ribatski, J. M. Jabardo, Experimental study of nucleate boiling of halocarbon refrigerants on cylindrical surfaces, Int. J. Heat Mass Tran. 46 (23) (2003) 4439-4451.

[4]      F. Ramstorfer, H. Steiner, G. Brenn, C. Kormann, F. Rammer, Subcooled Boiling Flow Heat Transfer From Plain and Enhanced Surfaces in Automotive Applications, J. Heat Transfer 130 (1) (2008) 011501.

[5]      D. Gorenflo, State of the art in pool boiling heat transfer of new refrigerants, Int. J. Refrig. 24 (1) (2001) 6-14.

[6]      J. M. S. Jabardo, G. Ribatski, E. Stelute, Roughness and surface material effects on nucleate boiling heat transfer from cylindrical surfaces to refrigerants R-134a and R-123, Exp. Therm. Fluid Sci. 33 (4) (2009) 579-590.

[7]      K. Robinson, N. Campbell, J. Hawley, D. Tilley, A Review of Precision Engine Cooling, Society of Automotive Engineering 01-0578 (1999).

[8]      A. Luke, Pool boiling heat transfer from horizontal tubes with different surface roughness, Int. J. Refrig. 20 (8) (1997) 561-574.

[9]      C. Martin-Callizo, B. Palm, W. Owhaib, Subcooled flow boiling of R-134a in vertical channels of small diameter, Int. J. Multiphas. Flow 33 (8) (2007) 822-832.

[10]     M. R. Özdemir, A. Kaya, A. Koşar, Low Mass Quality Flow Boiling in Microtubes at High Mass Fluxes, J. Thermal Sci. Eng. Appl. 3 (4) (2011) 41001.

[11]     A. Kaya, R. Demiryürek, E. Armagan, G. Ozaydin-Ince, M. Sezen, A. Kosar, Boiling heat transfer enhancement in mini/microtubes via polyhydroxyethylmethacrylate (pHEMA) coatings on inner microtube walls at high mass fluxes, J. Micromech. Microeng. 23 (11) (2013) 115017.

[12]     A. Kaya, M. R. Özdemir and A. Koşar, High mass flux flow boiling and critical heat flux in microscale, Int. J. Therm. Sci. 65 (2013) 70-78.

[13]    T. Çikim, E. Armagan, G. O. Ince, A. Kosar, Flow boiling enhancement in microtubes with crosslinked pHEMA Coatings and the Effect of Coating Thickness, J. Heat Transfer 136 (8) (2014) 81504.

[14]    P. Berenson, Experiments on pool-boiling heat transfer, Int. J. Heat Mass Tran. 5 (10) (1962) 985-999.

[15]    P. J. Marto, W. M. Rohsenow, Effect of surface conditions on nucleate pool boiling of sodium, J. Heat Transfer 88 (2) (1965) 196-203.

[16]    F. Tachibana, M. Akiyama, H. Kawamura, Non-Hydrodynamic Aspects of Pool Boiling Burnout, J. Nucl. Sci. Technol. 4 (3) (1967) 121-130.

[17]    G. Guglielmini, E. Nannei, On the effect of heating wall thickness on pool boiling burnout, Int. J. Heat Mass Tran. 19 (9) (1976) 1073-1075.

[18]    I. Golobic, A. E. Bergles, Effects of heater-side factors on the saturated pool boiling critical heat flux, Exp. Therm. Fluid Sci. 15 (1) (1997) 43-51.

[19]    M. Arik, A. Bar-Cohen, Effusivity-based correlation of surface property effects in pool boiling CHF of dielectric liquids, Int. J. Heat Mass Tran. 46 (20) (2003) 3755-3764.

[20]    V. Sernas, F. Hooper, The initial vapor bubble growth on a heated wall during nucleate boiling, Int. J. Heat Mass Tran. 12 (12) (1969) 1627-1639.

[21]    H. Unal, Maximum bubble diameter, maximum bubble-growth time and bubble-growth rate during the subcooled nucleate flow boiling of water up to 17.7 MN-m2, Int. J. Heat Mass Tran. 19 (1976) 643-649.

[22]    R. Benjamin, A. Balakrishnan, Nucleate pool boiling heat transfer of pure liquids at low to moderate heat fluxes, Int. J. Heat Mass Tran. 39 (12) (1996) 2495-2504.

[23]    R. J. Benjamin, A. R. Balakrishnan, Nucleation site density in pool boiling of saturated pure liquids: Effect of surface microroughness and surface and liquid physical properties, Exp. Therm. Fluid Sci. 15 (1997) 32-42.

[24]    W. Rohsenow, A method of correlating heat transfer data for surface boiling of liquids, Trans. ASME 74 (1952) 969-976.

[25]    L. Sterman, Y. Vilemas, The influence of the state of heating surface on heat transfer at boiling, Int. J. Heat Mass Tran. 11 (2) (1968) 347-351.

[26]    S. R. Chowdhury, R. Winterton, Surface effects in pool boiling, Int. J. Heat Mass Tran. 28 (10) (1985) 1881-1889.

[27]    N. Kolev, How accurately can we predict nucleate boiling?, Exp. Therm. Fluid Sci. 10 (3) (1995) 370-378.

[28]    K. T. Hong, H. Imadojemu, R. L. Webb, Effects of oxidation and surface roughness on contact angle, Exp. Therm. Fluid Sci. 8 (4) (1994) 279-285.

[29]    C. Y. Lee, B. J. Zhang, K. J. Kim, Influence of heated surfaces and fluids on pool boiling heat transfer, Exp. Therm. Fluid Sci. 59 (0) (2014) 15-23.

[30]    M. Cooper, Heat Flow Rates in Saturated Nucleate Pool Boiling-A Wide-Ranging Examination Using Reduced Properties 16, Elsevier, 1984, pp. 157-239.

[31]    L. Zou, B. G. Jones, Heating surface material's effect on subcooled flow boiling heat transfer of R134a, Int. J. Heat Mass Tran. 58 (2013) 168-174.

[32]    I. Pioro, W. Rohsenow, S. Doerffer, Nucleate pool-boiling heat transfer. I: review of parametric effects of boiling surface, Int. J. Heat Mass Tran. 47 (23) (2004) 5033-5044.

[33]    I. Pioro, W. Rohsenow, S. Doerffer, Nucleate pool-boiling heat transfer. II: assessment of prediction methods, Int. J. Heat Mass Tran. 47 (23) (2004) 5045-5057.

[34]    M.-G. Kang, Effect of surface roughness on pool boiling heat transfer, Int. J. Heat Mass Tran. 43 (22) (2000) 4073-4085.

[35]    J. P. McHale, S. V. Garimella, Bubble nucleation characteristics in pool boiling of a wetting liquid on smooth and rough surfaces, Int. J. Multiphas. Flow 36 (2010) 249-260.

[36]     A. Luke, Preparation and analysis of different roughness structures for evaporator tubes, Heat Mass Transfer 45 (7) (2009) 909-917.

[37]     S. Chatpun, M. Watanabe, M. Shoji, Experimental study on characteristics of nucleate pool boiling by the effects of cavity arrangement, Exp. Therm. Fluid Sci. 29 (1) (2004) 33-40.

[38]     E. Pike-Wilson, T. Karayiannis, Flow boiling of R245fa in 1.1mm diameter stainless steel, brass and copper tubes, Exp. Therm. Fluid Sci. 59 (2014) 166-183.

[39]     J. P. McHale, S. V. Garimella, Nucleate boiling from smooth and rough surfaces - Part 2: Analysis of surface roughness effects on nucleate boiling, Exp. Therm. Fluid Sci. 44 (2013) 439-455.

[40]     M. Arik, A. Koşar, H. Bostanci, A. Bar-Cohen, Pool Boiling Critical Heat Flux in Dielectric Liquids and Nanofluids, in Adv. Heat Transfer 43, Elsevier, 2011, pp. 1-76.

[41]     J. C. Chen, Correlation for boiling heat transfer to saturated fluids in convective Flow, Ind. Eng. Chem. Proc. DD. 5(3) (1966) 322-329.

[42]     I. Pioro, Experimental evaluation of constants for the Rohsenow pool boiling correlation, Int. J. Heat Mass Tran. 42 (11) (1999) 2003-2013.

[43]     J. M. S. Jabardo, E. F. da Silva, G. Ribatski, S. F. de Barros, Evaluation of the Rohsenow correlation through experimental pool boiling of halocarbon refrigerants on cylindrical surfaces, J. Braz. Soc. Mech. Sci. Eng. 26 (2004) 218-230.

[44]     K. Gungor, R. Winterton, A general correlation for flow boiling in tubes and annuli, Int. J. Heat Mass Tran. 29 (3) (1986) 351-358.

[45]     K. Stephan, H. Auracher, Correlations for nucleate boiling heat transfer in forced convection, Int. J. Heat Mass Tran. 24 (1) (1981) 99-107.

[46]     Z. Liu, R. Winterton, A general correlation for saturated and subcooled flow boiling in tubes and annuli, based on a nucleate pool boiling equation, Int. J. Heat Mass Tran. 34 (11) (1991) 2759-2766.

[47]     M. Shah, Chart correlation for saturated Boiling Heat Transfer: Equations and Further Study, ASHRAE J. 88 (1982) 165-196.

[48]     A. Torregrosa, A. Broatch, P. Olmeda, O. Cornejo, Experiments on subcooled flow boiling in I.C. engine-like conditions at low flow velocities, Exp. Therm. Fluid Sci. 52 (2014) 347-354.

[49]     D. Gorenflo, D. Kenning, Pool Boiling, Second English edition ed., V. D. I. V. V. und Chemieingenieurwesen (GVC), Springer-Verlag, 2010, pp. 757-792.

[50]     D. Gorenflo, P. Sokol, Prediction method of pool boiling heat transfer with cryogenic liquids, Int. J. Refrig. 11 (5) (1988) 315-320.

[51]     D. Gorenflo, P. Sokol, S. Caplanis, Pool boiling heat transfer from single plain tubes to various hydrocarbons, Int. J. Refrig. 13 (5) (1991) 286-292.

[52]     D. Gorenflo, U. Chandra, S. Kotthoff, A. Luke, Influence of thermophysical properties on pool boiling heat transfer of refrigerants, Int. J. Refrig. 27 (5) (2004) 492-502.

[53]     D. Gorenflo, S. Kotthoff, Review on pool boiling heat transfer of carbon dioxide, Int. J. Refrig. 28 (8) (2005) 1169-1185.

[54]     S. Kotthoff, D. Gorenflo, Pool boiling heat transfer to hydrocarbons and ammonia: A state-of-the-art review, Int. J. Refrig. 31 (4) (2008) 573-602.

[55]     D. Gorenflo, E. Baumhagger, G. Herres, S. Kotthoff, Prediction methods for pool boiling heat transfer: A state-of-the-art review, Int. J. Refrig. 43 (2014) 203-226.

[56]     G. Celata, M. Cumo, D. Gallo, A. Mariani, G. Zummo, A photographic study of subcooled flow boiling burnout at high heat flux and velocity, Int. J. Heat Mass Tran. 50 (2007) 283-291.

[57]     F. Ramstorfer, H. Steiner, G. Brenn, Effect of the vapor phase on the near-wall velocity field in subcooled boiling flow, in 6th International Conference on Multiphase Flow, Leipzig, 9-13 July 2007.

[58]    G. Ribatski, J. M. S. Jabardo, E. F. da Silva, Modeling and experimental study of nucleate boiling on a vertical array of horizontal plain tubes, Exp. Therm. Fluid Sci. 32 (8) (2008) 1530-1537.

[59]    F. Incropera, D. Dewitt, T. Bergman, A. Lavine, Fundamentals of Heat and Mass Transfer, 6th ed., John Wiley & Sons, 2007.

[60]    W. H. McAdams, W. E. Kennel, C. S. Minden, R. Carl, P. M. Picornell, J. E. Dew, Heat transfer at high rates to water with surface boiling, Ind. Eng. Chem. 41 (9) (1949) 1945-1953.

[61]    V. H. Del Valle, D. Kenning, Subcooled flow boiling at high heat flux, Int. J. Heat Mass Tran. 28 (10) (1985) 1907-1920.

[62]    H. Steiner, A. Kobor, L. Gebhard, A wall heat transfer model for subcooled boiling flow, Int. J. Heat Mass Tran. 48 (2005) 4161-4173.

[63]    K. Robinson, J. Hawle, N. Campbell, Experimental and modelling aspects of flow boiling heat transfer for application to internal combustion engines, Proc. Instn. Mech. Engrs. Part D: J. Automobile Eng. 217 (10) (2003) 877-889.

[64]    S. Kutateladze, Boiling heat transfer, Int. J. Heat Mass Tran. 4 (0) (1961) 31-45.

[65]    D. Steiner, J. Taborek, Flow Boiling Heat Transfer in Vertical Tubes Correlated by an Asymptotic Model, Heat Transfer Eng. 13 (2) (1992) 43-69.

 [66]    M. Shah, A general correlation for heat transfer during subcooled boiling in pipes and annuli, ASHRAE Trans. 83 (1977) 205-217.

[67]    S. Kandlikar, Heat transfer characteristics in partial boiling, fully developed boiling, and significant void flow regions of subcooled flow boiling, J. Heat Transfer 120 (2) (1998) 395-401.

[68]    M. M. E. Gollin, C. Stinson, Comparative Performance of Ethylene Glycol/Water and Propylene Glycol/Water Coolants in the Convective and Forced Flow Boiling Regimes, Society of Automotive Engineering 950464 (1995).

[69]    R. D. Boyd, M. Strahan, P. Cofie, A. Ekhlassi, R. Martin, High heat flux removal using water subcooled flow boiling in a single-side heated circular channel, Int. J. Heat Mass Tran. 46 (21) (2003) 4105-4117.

[70]    H. Lee, A. O'Neill, Comparison of Boiling Curves between a Standard S.I. Engine and a Flow Loop for a Mixture of Ethylene Glycol and Water,  Society of Automotive Engineering 01-1231 (2006).

[71]    H. Lee, Heat Transfer Predictions using the Chen Correlation on Subcooled Flow Boiling in a Standard IC Engine, Society of Automotive Engineering 01-1530 (2009).

**List of figures**

**List of tables**

**Fig. 1 Experimental test facility.**
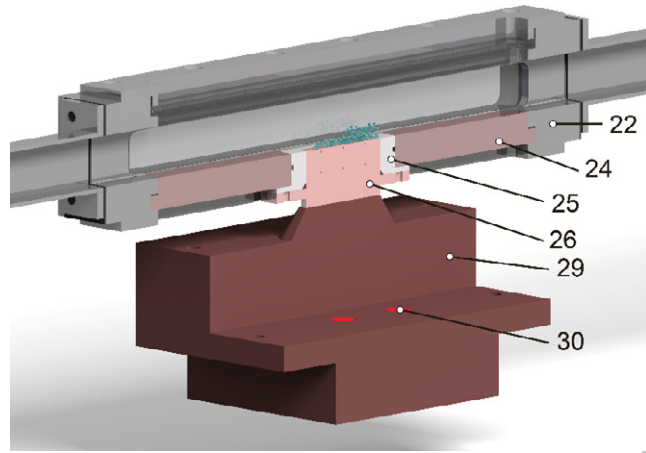
**Fig. 2 Section of study**.

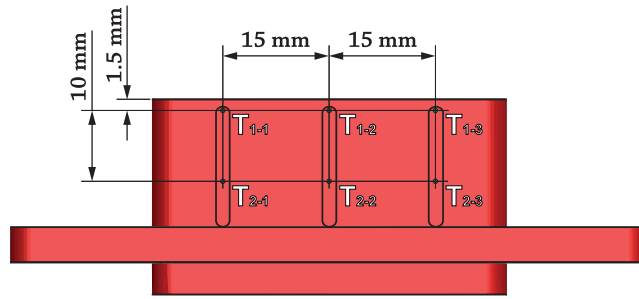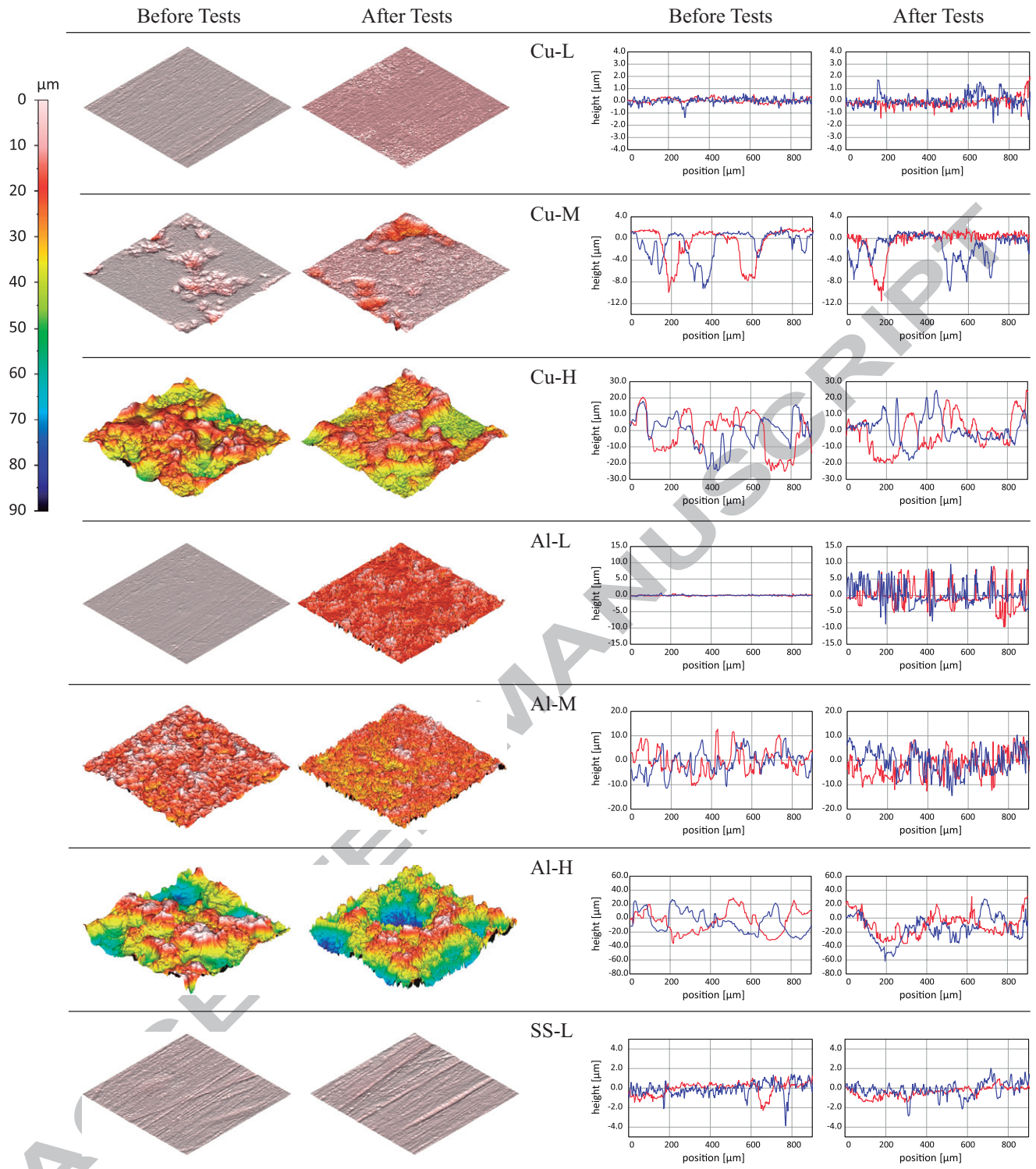**Fig. 3 Location of the thermocouples in the test part.**

**Fig. 4 Topography (left), random cross section profile along X axis (right-red) and random cross section profile along Y axis (right-blue) for each test part analysed before and after test.** The topography comprises an area of 0.5x0.5 mm, and the cross section profile comprises a length of 0.9 mm.
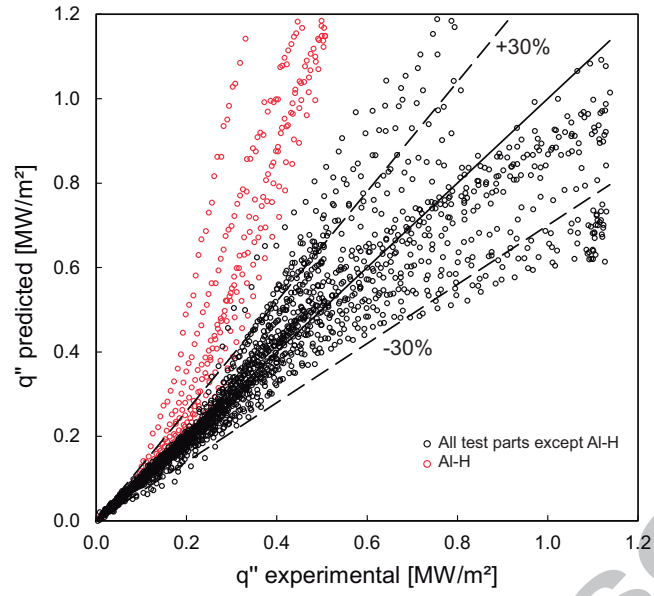
**Fig. 5 Model performance.** Red points correspond to roughest aluminium part [Al-H].
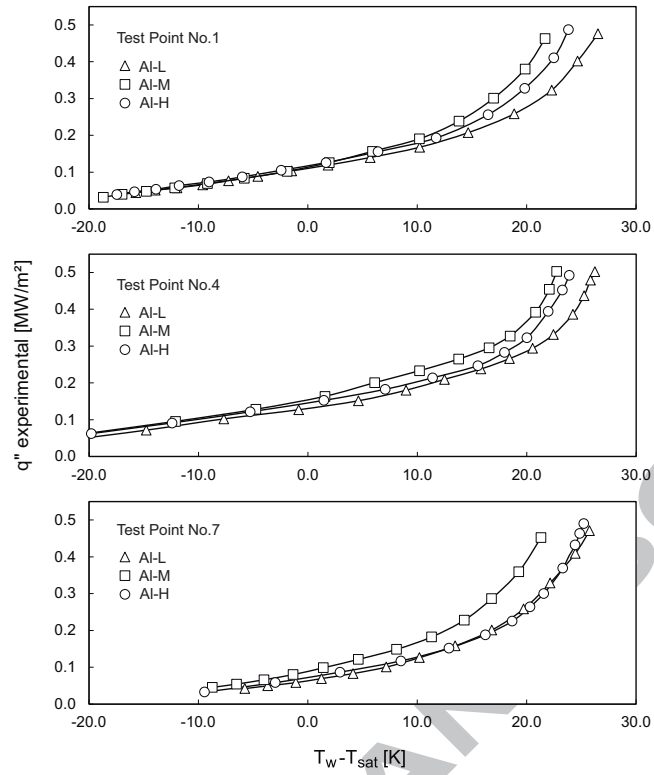
**Fig. 6 Experimental results for aluminium test parts and 1, 4 and 7 test points.**
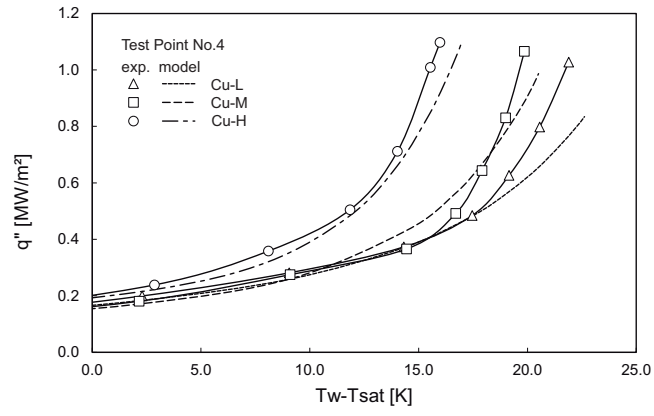
**Fig. 7 Experimental results and model output for cooper test parts.** Test point no. 4.
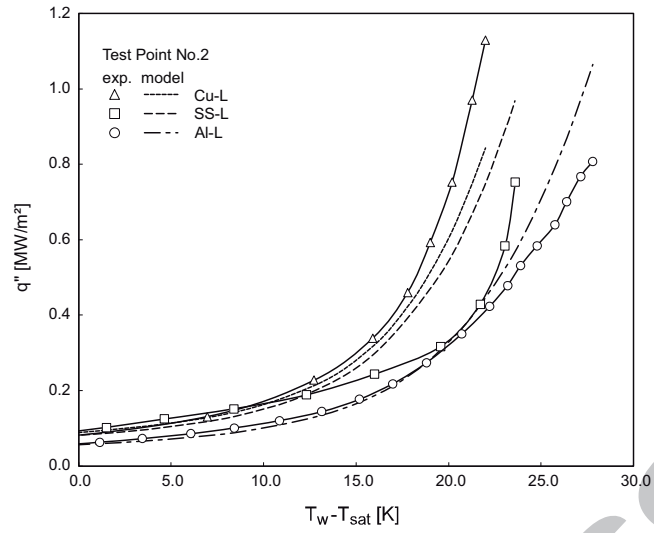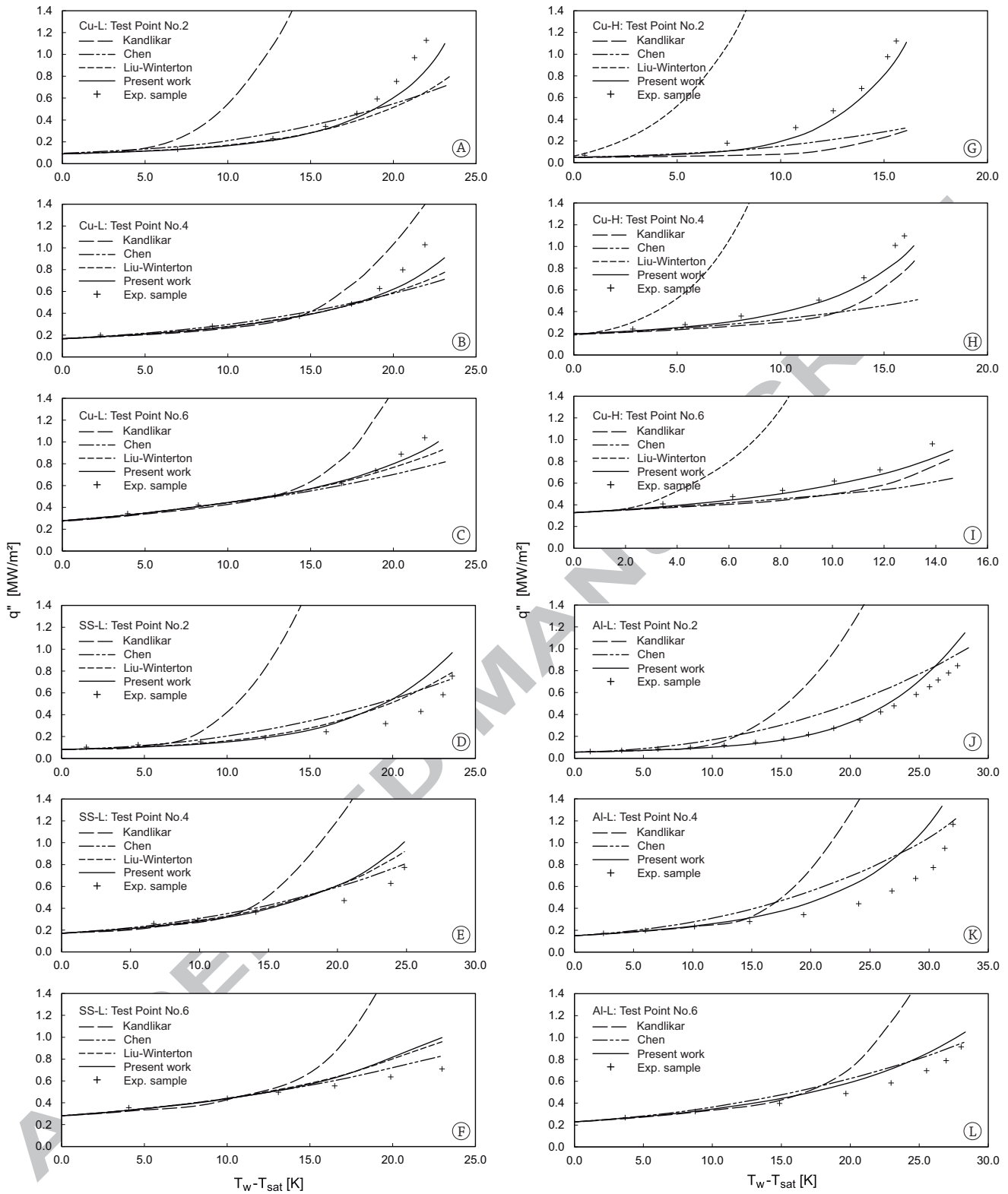
**Fig. 8 Experimental results and model output for aluminium, cooper and s. steel low roughness test parts.** Test point no. 2.

**Fig. 9 Kandlikar [67], Chen [41], Liu-Winterton [46] and presented model [Eq. (15)] graphical output for Cu-L, Cu-H, SS-L and Al-L parts.** Experimental points are symbolized by '+' whereas the different lines show the output of the models.

**Table 1**
Reference point for VDI pool boiling model and water as refrigerant.

| Designation | Value |
|---|---|
| $h_{nb,0}$ | 5.60  $kW \cdot m^{-2} \cdot K^{-1}$ |
| $q_0^{"}$ | 20  $kW \cdot m^{-2}$ |
| $P_{f,ref}$ | 1  $\mu m^{-1} \cdot K^{-1}$ |
| $R_{a,0}$ | 0.4  $\mu m$ |

**Table 2**
Summary of test parts.

| Designation | Material | Surface finish | $R_{a,\,min}$ AT [μm] | $R_{a,\,max}$ AT [μm] | Sa BT [μm] | Sa AT [μm] | Effusivity@130°C [J·m$^{-2}$·K$^{-1}$·s$^{-0.5}$] |
|---|---|---|---|---|---|---|---|
| Cu-L | Copper | Sandpaper | 0.12 | 0.61 | 0.18 | 0.41 | 37,463 |
| Cu-M | Copper | EDM+sandpaper | 0.24 | 2.52 | 2.05 | 1.48 | 37,463 |
| Cu-H | Copper | EDM | 1.82 | 7.42 | 7.47 | 7.33 | 37,463 |
| Al-L | Aluminium | Sandpaper | 0.48 | 3.87 | 0.38 | 2.09 | 17,368 |
| Al-M | Aluminium | EDM | 2.06 | 5.00 | 3.38 | 4.17 | 17,368 |
| Al-H | Aluminium | EDM | 4.16 | 12.07 | 11.29 | 11.84 | 17,368 |
| SS-L | Copper+AISI-316 | Rolled | 0.11 | 0.61 | 0.44 | 0.41 | 35,100 |

**Table 3**
Test points.

| Designation | Bulk temp. [°C] | Bulk velocity [m·s$^{-1}$] | Pressure [kPa] | Mass flux [kg·s$^{-1}$·m$^2$] |
|---|---|---|---|---|
| 1 | 76.5 | 0.5 | 150 | 487.0 |
| 2 | 85.0 | 0.1 | 150 | 96.9 |
| 3 | 85.0 | 0.5 | 115 | 484.4 |
| 4 | 85.0 | 0.5 | 150 | 484.4 |
| 5 | 85.0 | 0.5 | 190 | 484.4 |
| 6 | 85.0 | 0.9 | 150 | 872.0 |
| 7 | 93.5 | 0.5 | 150 | 481.6 |

**Table 4**

$h_{nb}$ calculation for the presented model.

$$h_{nb} = 6.457 \cdot F_q \cdot F_{p*} \cdot F_{wr} \cdot F_{wm} \quad \left[ kW \cdot m^{-2} \cdot K^{-1} \right]$$

$$F_q = \left( \frac{q''}{20 \cdot 10^3} \right)^{0.9 - 0.3 \, p^{*0.15}}$$

$$F_{p*} = 1.73 \, p^{*0.27} + 6.1 \, p^{*2} + 0.68 \frac{p^{*2}}{1 - p^{*2}}$$

$$F_{wr} = \left( \frac{S_a}{0.4} \right)^{2/15} \quad S_a \ in \ \mu m$$

$$F_{wm} = \left( \frac{\rho \cdot c \cdot k|_w}{37,463} \right)^{0.25}$$

**Table 5**

Selected models comparative results. RMS Error, percent value.

| Designation | Chen [41] | Shah [66] | Liu-Winterton [46] | Kandlikar [67] | Presented model [Eq. (15)] |
|---|---|---|---|---|---|
| Cu-L | 20 % | 50 % | 19 % | 195 % | 17 % |
| Cu-M | 27 % | 35 % | 104 % | 17 % | 15 % |
| Cu-H | 40 % | 38 % | 518 % | 42 % | 20 % |
| Al-L | 33 % | 56 % | - | 151 % | 19 % |
| Al-M | 27 % | 50 % | - | 184 % | 16 % |
| Al-H | 52 % | 30 % | - | 61 % | 106 % |
| SS-L | 24 % | 89 % | 25 % | 366 % | 26 % |

Highlights

- An experimental work is developed on the nucleate boiling behaviour of different surfaces.
- A new model for subcooled flow boiling of water at low pressure has been proposed.
- The model takes into account wall material and roughness effects.
- The model is based on a non-directional parameter (Sa).
- The model performs reasonably well in contrast to other spread-used models.